Supporting Information for

Di-lacunary $[In_6S_{15}]^{12-}$ cluster: the building block of a highly negatively charged framework for superior Sr^{2+} adsorption capacities

Kai-Yao Wang,[*a] *Meng Sun,*[a] *Dong Ding,*[a] *Hua-Wei Liu,*[a] *Lin Cheng,*[b] *Cheng Wang*[a]

[a]Tianjin Key Laboratory of Advanced Functional Porous Materials, Institute for New Energy Materials and Low-Carbon Technologies, School of Materials Science and Engineering, Tianjin University of Technology, Tianjin 300384, P. R. China.
[b]College of Chemistry, Tianjin Normal University, Tianjin 300387, P. R. China.

1. Materials and General Methods.

All reagents and solvents employed were commercially available and were used without further purification. Elemental analysis on H, C and N were performed on an Elementar Vario EL cube instrument. Powder X-ray diffraction (XRD) patterns were collected in the angular range of 2θ = 5-90 ° on the Rigaku XtaLab PRO single-crystal X-ray diffractometer using the powder tool (Cu-*K*α radiation, λ = 1.5418 Å). Scanning electron microscopy (SEM) and Energy-dispersive spectroscopy (EDS) were performed on a FEI Quanta FEG 250 scanning electron microscope. FTIR spectra (KBr pellets) were measured on a PerkinElmer Frontier Mid-IR FTIR spectrometer. Solid-state UV/vis reflectance spectra were performed in the wavelength range of 200−2000 nm using a PerkinElmer Lambda 750 UV/vis spectrophotometer, and a $BaSO_4$ plate was used as a standard (100% reflectance). The absorption $F(R)$ data were calculated from reflectance spectra by using the Kubelka-Munk function: $F(R) = (1-R)^2/2R$, where R is the reflectance.[1] ^1H and ^{13}C NMR spectra of the compound dissolved in mixed HCl (1 M)/D_2O were recorded on a Bruker Avance III 400 instrument using 5 mm tubes at room temperature. The concentrations of metal ions in the process of ion exchange were measured by a ThermoFisher iCAP RQ inductively coupled plasma mass spectrometer (ICP-MS). X-ray photoelectron spectroscopy (XPS) was performed on a Kratos Axis Ultra DLD X-ray photoelectron spectrometer. Elemental analysis (H, C, and N) were performed on an Elementar Vario EL cube instrument. **InS-1** was irradiated at 1.2 kGy/h for a dose of 100 kGy in the ^{60}Co γ irradiation experiment and at 20 kGy/h for two different doses of 100 and 200 kGy in the β irradiation experiment. β irradiation was conducted using electron beams (10 MeV) that were provided by an electron accelerator located in CGN Dasheng Electron Accelerator Co., Ltd., in Jiangsu Province, China.

2. Synthesis.

$[CH_3CH_2NH_3]_6In_6S_{12}$ (**InS-1**). A mixture of indium(III) chloride (0.111 g, 0.5 mmol), trithiocyanuric acid (0.221 g, 1.2 mmol), 2.5 mL ethylamine ethanol solution (30~35%) and 1 mL ethanol was sealed in a stainless steel reactor with a 20 mL Teflon liner and heated at 160 °C for 4 days. After cooling to room temperature by natural ventilation, the product was washed with distilled water and then dried in the air. A 0.0521 g portion of pure plate-like colorless crystals of **InS-1** were collected in a yield of 46.1 % based on In. Anal. Calcd for $C_{12}H_{48}In_6N_6S_{12}$ (1350.20): C, 10.67; H, 3.58; N, 6.22. Found: C, 9.48; H, 3.39; N, 5.93.

3. Crystallography

Indexing and data collection of one **InS-1** single crystal was performed on a Rigaku XtaLab PRO diffractometer with graphite-monochromated Mo *K*α radiation (λ

= 0.71073 Å) at 293 K. The absorption corrections were applied using a multi-scan technique. The In and S atoms in the structure were solved by a direct method using SHELXS-97, and successive Fourier syntheses (SHELXL2014) revealed the remaining atoms.[2] Refinements were conducted by full matrix least squares against $|F|^2$ using all data. All of the In, S, C and N atoms were refined by anisotropic displacement parameters. The hydrogen atoms around C and N atoms were obtained with idealized geometries. SQUEEZE was used to remove the contributions of disordered ethylammonium cations. The relevant crystallographic data and structure refinement details are shown in Table S1.

4. Ion-Exchange Experiments

A typical ion exchange experiment was conducted in a batch method at a *V*/*m* ratio of 1000 mL g^{-1} in a covered 20 mL vial. A quantity of 20 mg of **InS-1** was added to 20 mL of $SrCl_2 \cdot 6H_2O$ aqueous solution with predetermined Sr^{2+} concentrations, and the mixture was kept at room temperature with constant stirring for 24 h to reach the adsorption equilibrium. Then the exchanger was isolated by filtration (through filtration paper, Whatman 102) and washed several times with deionized water and dried in the air. Powder XRD, XPS, FTIR, UV/vis, EDS and elemental mapping measurements were performed on the solid sample obtained from 0.1 M $SrCl_2 \cdot 6H_2O$ solution (i.e. **InS-1Sr**). The filtered solutions were diluted by 2% HNO_3 into a suitable scope (below 150 ppb for metal ions) before the concentration of Sr^{2+} was determined using ICP-MS.

The Sr^{2+} ion exchange kinetics studies were conducted for various contact time (0-2880 min) in the solution containing 5.68 ppm Sr^{2+}. The ion exchange isotherms were studied in solutions with initial concentrations of Sr^{2+} ranging from 2 to 658 ppm for 24 h contact time.

The individual Sr^{2+} ion exchange experiments at different pH and salt concentrations were carried out as follows. The required pH values (range from 1 to 14) were achieved by diluting the solution of Sr^{2+} (600 ppm) with HCl and NaOH solution to 5.39-5.84 ppm. The experiments were carried out for 24 h contact time, and the pH values of the solutions after ion exchange process were also measured. The effects of coexisting cations were determined by dissolving required amount of NaCl, KCl, $MgCl_2$, $CaCl_2$ in the solution of Sr^{2+} (5.30-5.68 ppm), and these experiments were conducted at room temperature for 24 h contact time.

The Sr^{2+}-exchanged product with saturated adsorption, i.e. **InS-1Sr**, was used in the elution experiment. The **InS-1Sr** (20 mg) sample was soaked in 20 mL of 0.5 M KCl solution with constant stirring for 24 h. Then the solid product (**InS-1K**) was separated by filtration (through filtration paper, Whatman 102) and washed several times with deionized water and dried in air. The product was checked by powder XRD, EDS and elemental mapping.

5. Equations for ion exchange analysis:

(1) Pseudo-second-order kinetics model:

$$\frac{t}{q_t} = \frac{1}{k_2 q_e^2} + \frac{t}{q_e} \tag{1}$$

Here, k_2 (g mg^{-1} min^{-1}) is the pseudo-second-order rate constant of the kinetics model, and the q_t and q_e (mg g^{-1}) represents the mass of a metal ion adsorbed per unit weight of adsorbent at time t (min) and at equilibrium.

(2) The amount of target ions adsorbed on ion exchangers at equilibrium (q, mg g^{-1}):

$$q = \frac{(C_0 - C_e)V}{m} \tag{2}$$

Here, C_0 (ppm) and C_e (ppm) are the initial and equilibrium concentrations of Sr^{2+} ion, V (mL) is the volume of the test solution, and m (g) is the mass of ion exchanger.

(3) Langmuir-Freundlich isotherm model[3]:

$$q = q_m \frac{(bC_e)^{1/n}}{1 + (bC_e)^{1/n}} \tag{3}$$

Here, b (L mg^{-1}) is the Langmuir constant, q_m (mg g^{-1}) is the maximum ion exchange capacity, and n is a parameter characterizing the system heterogeneity.

(4) Distribution coefficient K_d (mL g^{-1}):

$$K_d = \frac{V}{m} \frac{(C_0 - C_f)}{C_f} \tag{4}$$

Here, V (mL) is the volume of the test solution, and m (g) is the mass of ion exchanger, C_0 and C_f (ppm) are the initial and final concentration of the ion.

6. Tables

Table S1. Crystal data for **InS-1**.

Compound	**InS-1**
Empirical formula	$C_{12}H_{48}In_6N_6S_{12}$
Formula weight	1350.20
Crystal system	Monoclinic
Space group	$P2_1/n$
T/K	293(2)
λ/Å	1.54178
a/Å	9.7420(2)
b/Å	14.4225(3)
c/Å	28.1311(5)
α/°	90
β/°	93.409(2)
γ/°	90
V/Å^3	3945.54(14)
Z	4
D_c/Mg·m^{-3}	2.273
μ/mm^{-1}	33.637
F(000)	2592
Measured refls.	27422
Independent refls.	8031
R_{int}	0.0771
No. of parameters	244
GOF	1.049
R_1,[a] $wR_2[I > 2\sigma(I)]$	0.0920, 0.2606
R_1, wR_2 (all data)	0.1008, 0.2691

[a] $R_1 = \sum||Fo|-|Fc||/\sum|Fo|$, $wR_2 = \{\sum w[(Fo)^2-(Fc)^2]^2/\sum w[(Fo)^2]^2\}^{1/2}$

Table S2. Selected hydrogen-bonding data for **InS-1**.

D–H···A	d(D–H)	d(H···A)	d(D···A)	<(DHA)
N(1)–H(1A)···S(10)#4	0.89	2.43	3.291(17)	163.5
N(1)–H(1B)···S(8)	0.89	2.56	3.289(15)	139.2
N(2)–H(2A)···S(8)	0.89	2.40	3.275(14)	166.1
N(2)–H(2B)···S(11)#4	0.89	2.94	3.523(17)	125.0
N(2)–H(2B)···S(12)#1	0.89	2.87	3.337(14)	114.4
N(2)–H(2C)···S(2)#1	0.89	2.59	3.303(18)	138.1
N(3)–H(3A)···S(10)	0.89	2.93	3.379(19)	113.1
N(3)–H(3A)···S(12)	0.89	2.53	3.326(19)	149.9
N(3)–H(3B)···S(11)#5	0.89	2.72	3.496(19)	146.2
C(2)–H(2F)···S(4)	0.96	2.99	3.94(3)	174.1
C(3)–H(3D)···S(10)#4	0.97	2.95	3.73(4)	138.7
C(5)–H(5B)···S(3)#4	0.97	2.94	3.89(5)	164.7

Symmetry codes: #1 *x*-1, *y*, *z*; #2 -*x*+1/2, *y*-1/2, -*z*+1/2; #3 *x*+1, *y*, *z*; #4 -*x*+1/2, *y*+1/2, -*z*+1/2; #5 -*x*+3/2, *y*+1/2, -*z*+1/2.

Table S3. Summary of negative charge densities and ion exchange capacities for chalcogenide ion exchangers.

Ion exchangers	Anionic network	Negative charges (*N*)	Molecular mass of the anionic network (*M*)	Charge density (*N*/*M*) ($\times 10^{-3}$)	Exchanged cations and capacities (q_m, mg g^{-1})	Ref.
$(NH_4)_4In_{12}Se_{20}$	$[In_{12}Se_{20}]_n^{4n-}$	4	2957.0	1.35	Cs^+, Rb^+, Hg^{2+}, Pb^{2+}, Ag^+	[4]
$[(Me)_2NH_2]_{0.75}[Ag_{1.25}SnSe_3]$	$[Ag_{1.25}SnSe_3]_n^{0.75n-}$	0.75	490.4	1.53	Cs^+, Rb^+, NH_4^+	[5]
$[CH_3NH_3]_{0.75}Cu_{1.25}GeSe_3$ (CuGeSe-1)	$[Cu_{1.25}GeSe_3]_n^{0.75n-}$	0.75	389.0	1.93	Cs^+ (225.3)	[6]
$[H_3O]_3[Heta]_{4.2}[H_2dpp]_{0.3}[In_4Sn_{16}O_{10}S_{32}]$	$[In_4Sn_{16}O_{10}S_{32}]_n^{8n-}$	8	3544.7	2.26	Cs^+, Hg^{2+}, Pb^{2+}, Cd^{2+}	[7]
$[(CH_3CH_2CH_2)_2NH_2]_5In_5Sb_6S_{19}\cdot 1.45H_2O$	$[In_5Sb_6S_{19}]_n^{5n-}$	5	1913.9	2.61	Cs^+	[8]
$[CH_3NH_3]_{20}Ge_{10}Sb_{28}S_{72}\cdot 7H_2O$	$[Ge_{10}Sb_{28}S_{72}]_n^{20n-}$	20	6444.4	3.10	Cs^+	[9]
$[(CH_3)_2NH_2]_2Ga_2Sb_2S_7\cdot H_2O$ (SG: $P2_1$) $[Me_2NH_2]_2[Ga_2Sb_2S_7]\cdot H_2O$ (FJSM-GaS-1; SG: $P2_12_12_1$) $[Et_2NH_2]_2[Ga_2Sb_2S_7]\cdot H_2O$ (FJSM-GaS-2)	$[Ga_2Sb_2S_7]_n^{2n-}$	2	607.4	3.29	Cs^+ (164 ± 16 for FJSM-GaS-1) Sr^{2+} (80 ± 3 for FJSM-GaS-1) UO_2^{2+} (196 ± 56 for FJSM-GaS-1; 144 ± 12 for FJSM-GaS-2)	[10] [11]
$(Heta)_{9.5}(H_3O)_{2.5}[In_8Sn_{12}O_{10}S_{32}]\cdot 22H_2O$ (InSnOS)	$[In_8Sn_{12}O_{10}S_{32}]_n^{12n-}$	12	3529.1	3.40	Cs^+ (537.7 ± 4.49)	[12]
$K_{2x}Sn_{4-x}S_{8-x}$ (x = 0.65-1) (KTS-3)	$[Sn_{4-x}S_{8-x}]_n^{2xn-}$	1.3-2	633.4-580.6	2.05-3.44	Cs^+ (280 ± 11) Sr^{2+} (102 ± 5) UO_2^{2+} (287 ± 15)	[13]
$(Me_2NH_2)_{1.33}(Me_3NH)_{0.67}Sn_3S_7\cdot 1.25H_2O$ (FJSM-SnS)	$[Sn_3S_7]_n^{2n-}$	2	580.6	3.44	Cs^+ (409 ± 29) Sr^{2+} (65 ± 5) UO_2^{2+} (338.43) Eu^{3+} (139.82 ± 3.42) Tb^{3+} (147.05± 4.53) Nd^{3+} (126.70 ± 3.90)	[14] [15] [16]

Table S3. Summary of negative charge densities and ion exchange capacities for chalcogenide ion exchangers (continued).

Ion exchangers	Anionic network	Negative charges (*N*)	Molecular mass of the anionic network (*M*)	Charge density (*N*/*M*) ($\times 10^{-3}$)	Exchanged cations and capacities (q_m, mg g^{-1})	Ref.
$K_{2x}Mn_xSn_{3-x}S_6$ (x = 0.5-0.95) (KMS-1)	$[Mn_xSn_{3-x}S_6]_n^{2xn-}$	1-1.9	516.6-488.0	1.94-3.89	Cs^+ (226 ± 2)	[17]
					Sr^{2+} (77 ± 2)	[18]
					Hg^{2+} (377 ± 15)	[19]
					Pb^{2+} (319 ± 4)	[20]
					Cd^{2+} (329)	[21]
					Ni^{2+} (29 ± 1)	[22]
					UO_2^{2+} (380 ± 20)	
					Cu^{2+} (155)	
$[(Me)_2NH_2]_2[GeSb_2S_6]$	$[GeSb_2S_6]_n^{2n-}$	2	508.5	3.93	Cs^+	[23]
$K_6Sn[Zn_4Sn_4S_{17}]$	$[Zn_4Sn_5S_{17}]_n^{6n-}$	6	1400.3	4.28	Rb^+, Cs^+, NH_4^+	[24]
						[25]
$K_{2x}Mg_xSn_{3-x}S_6$ (x = 0.5-1) (KMS-2)	$[Mg_xSn_{3-x}S_6]_n^{2xn-}$	1-2	501.3-454.1	1.99-4.40	Cs^+ (531 ± 28)	[22]
					Sr^{2+} (87 ± 2)	
					Ni^{2+} (151 ± 8)	
$[NH_3CH_3]_4[In_4SbS_9SH]$	$[In_4SbS_9SH]_n^{4n-}$	4	902.7	4.43	Rb^+	[26]
$Na_5Zn_{3.5}Sn_{3.5}S_{13}\cdot 6H_2O$ (ZnSnS-1)	$[Zn_{3.5}Sn_{3.5}S_{13}]_n^{5n-}$	5	1061.3	4.71	Sr^{2+} (124.2 ± 21.2)	[27]
$[CH_3CH_2NH_3]_6In_6S_{12}$ (InS-1)	$[In_6S_{12}]_n^{6n-}$	6	1073.7	5.59	Sr^{2+} (105.35 ± 14.07)	This work

7. Figures

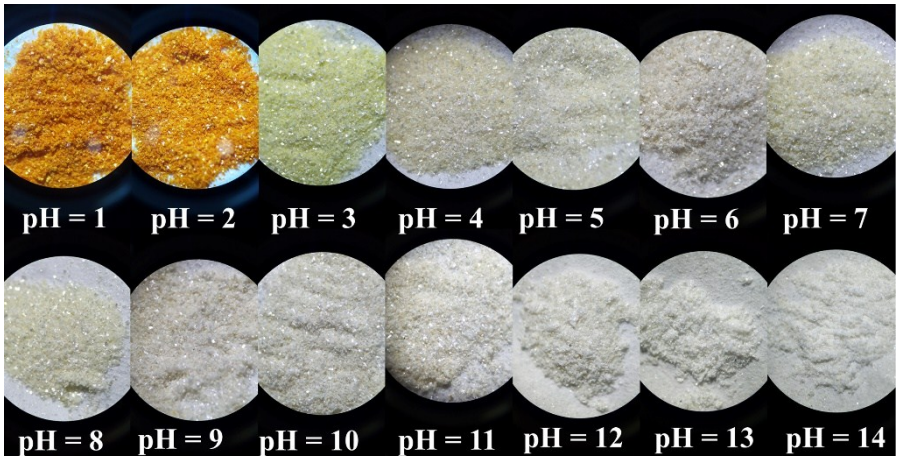

Figure S1. Photographs of the Sr^{2+}-exchanged products obtained from the test solutions with pH varying from 1 to 14 (C_0^{Sr} = 5.39-5.84 ppm; V/m = 1000 mL g^{-1}).

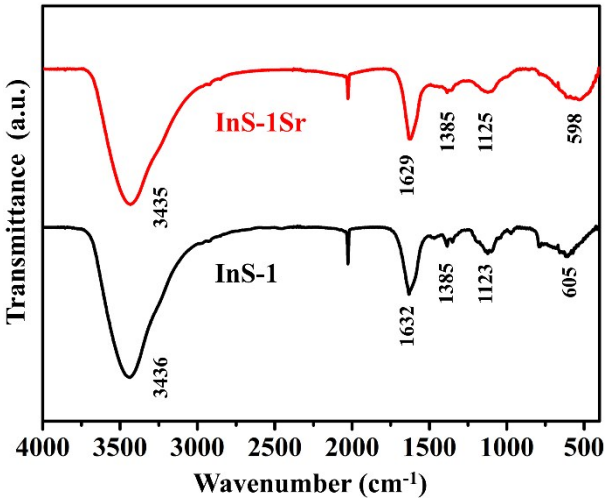

Figure S2. FTIR spectra of **InS-1** and **InS-1Sr** measured at room temperature on KBr pellets.

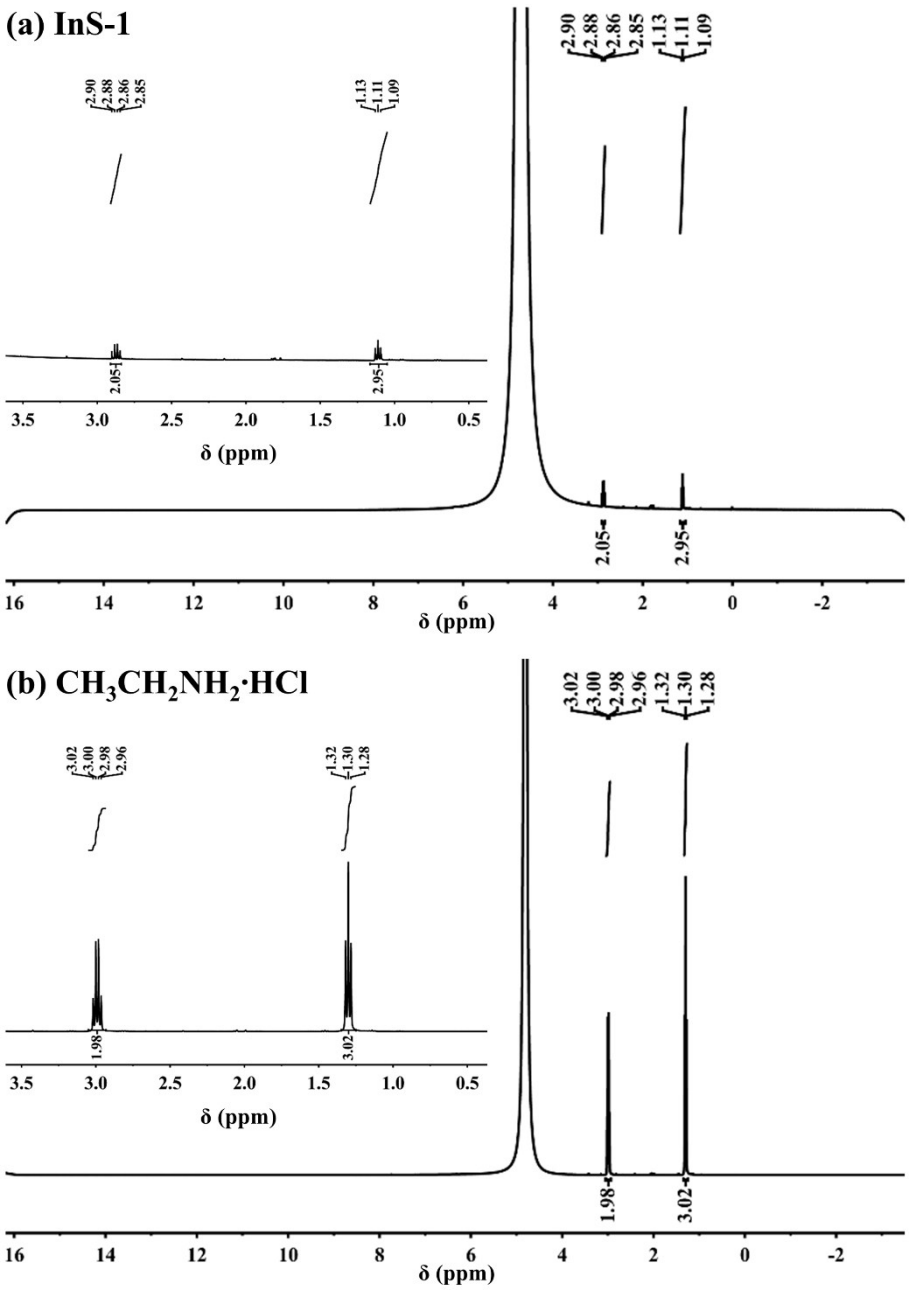

Figure S3. ^{1}H NMR spectra of (a) **InS-1** and (b) ethylamine hydrochloride dissolved in mixed HCl (1 M)/D_2O recorded at room temperature.

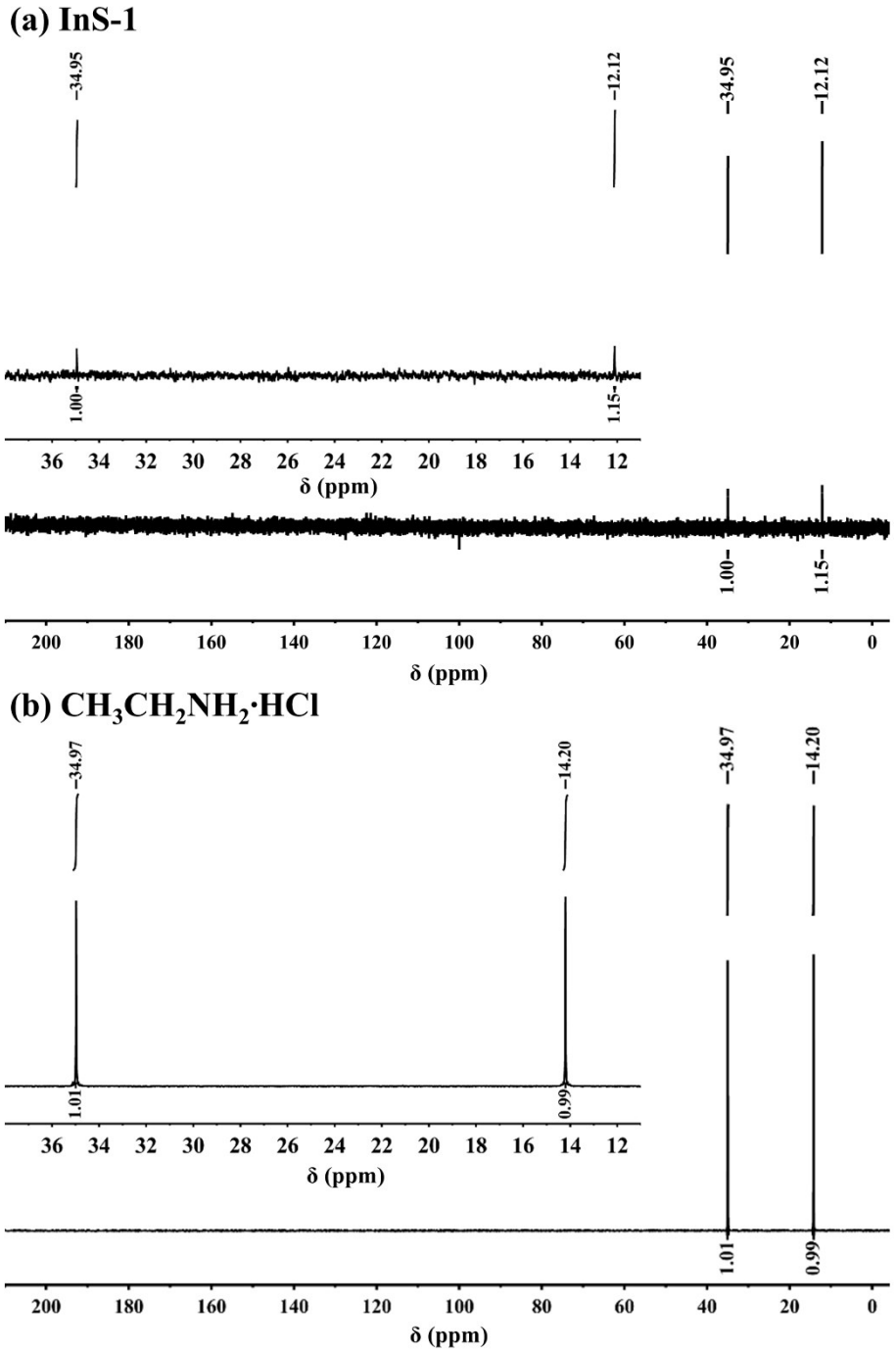

Figure S4. ^{13}C NMR spectra of (a) **InS-1** and (b) ethylamine hydrochloride dissolved in mixed HCl (1 M)/D_2O recorded at room temperature.

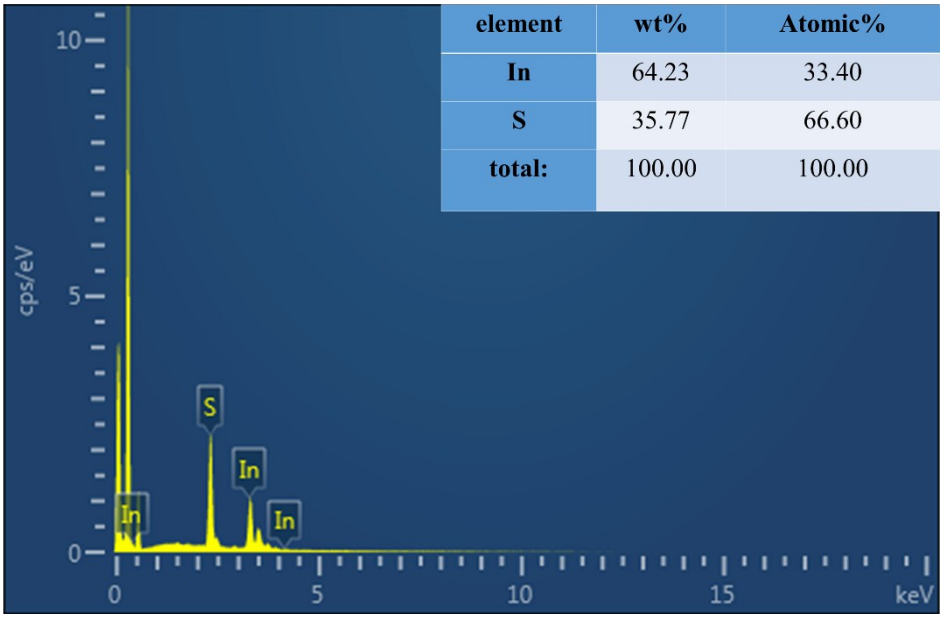

element	wt%	Atomic%
In	64.23	33.40
S	35.77	66.60
total:	100.00	100.00

Figure S5. EDS analysis on **InS-1**.

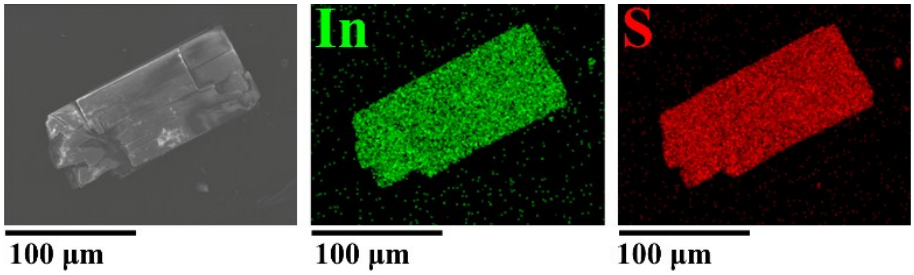

Figure S6. SEM image of **InS-1** and EDS elemental distribution maps of In and S.

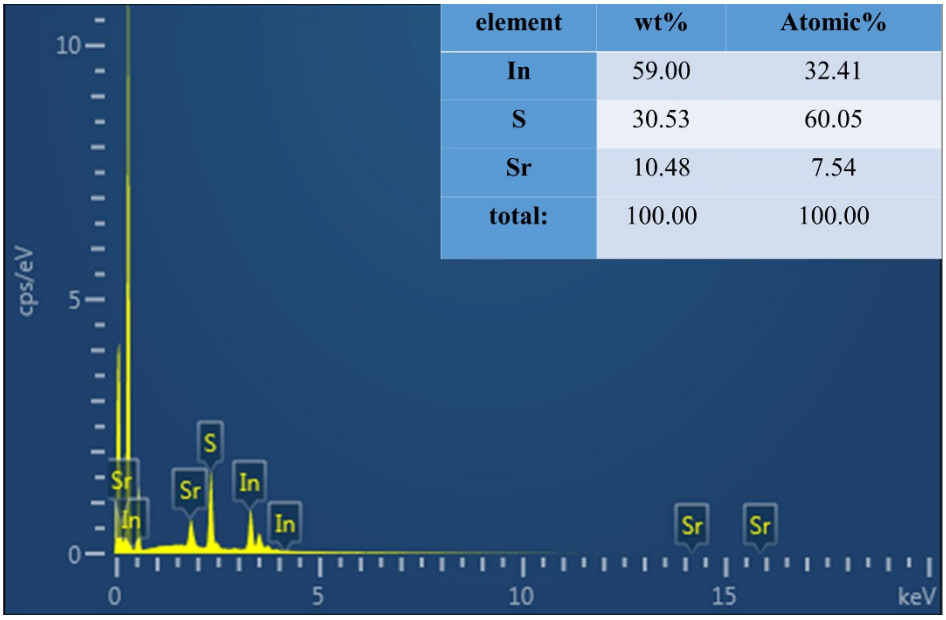

element	wt%	Atomic%
In	59.00	32.41
S	30.53	60.05
Sr	10.48	7.54
total:	100.00	100.00

Figure S7. EDS analysis on **InS-1Sr**.

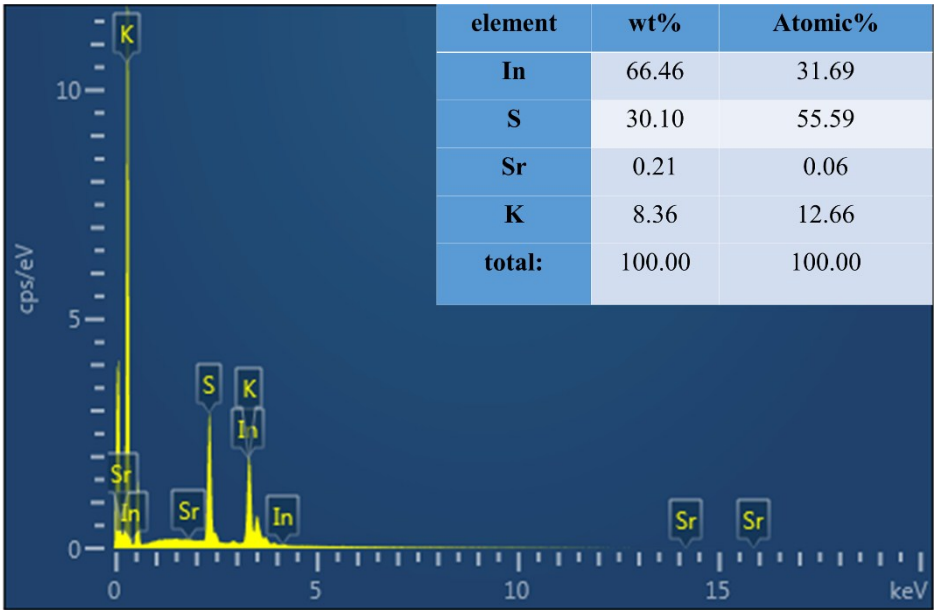

element	wt%	Atomic%
In	66.46	31.69
S	30.10	55.59
Sr	0.21	0.06
K	8.36	12.66
total:	100.00	100.00

Figure S8. EDS analysis on the eluted product **InS-1K**.

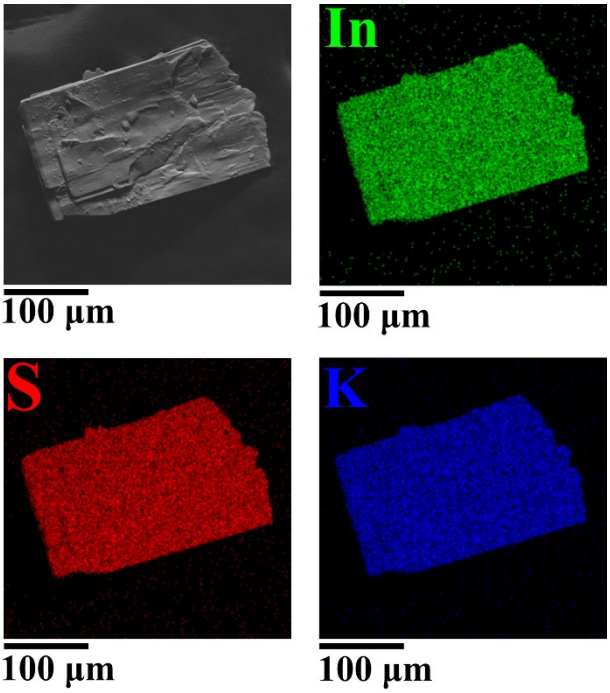

Figure S9. SEM image of the eluted product **InS-1K** and EDS elemental distribution maps for K, In and S. There is only trace Sr detected in the mapping measurement.

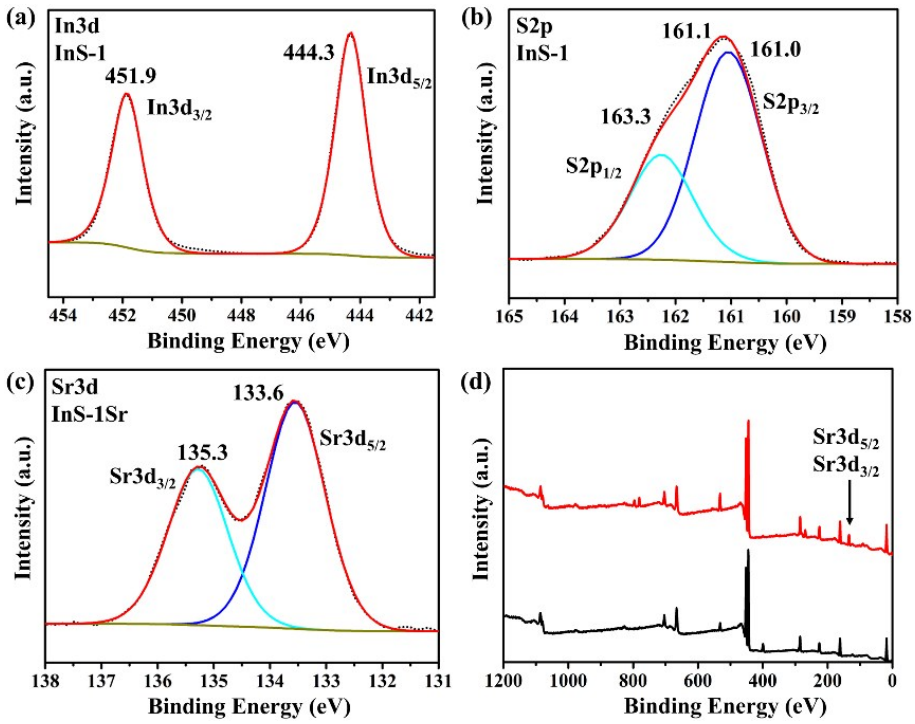

Figure S10. X-ray photoelectron spectra of (a) In, (b) S, for **InS-1** and (c) Sr for **InS-1Sr**. (d) Comparison of experimental survey spectra of the product before (black line) and after (red line) ion exchange. Black dotted and red solid lines represent experimental and overall fitting curves, respectively.

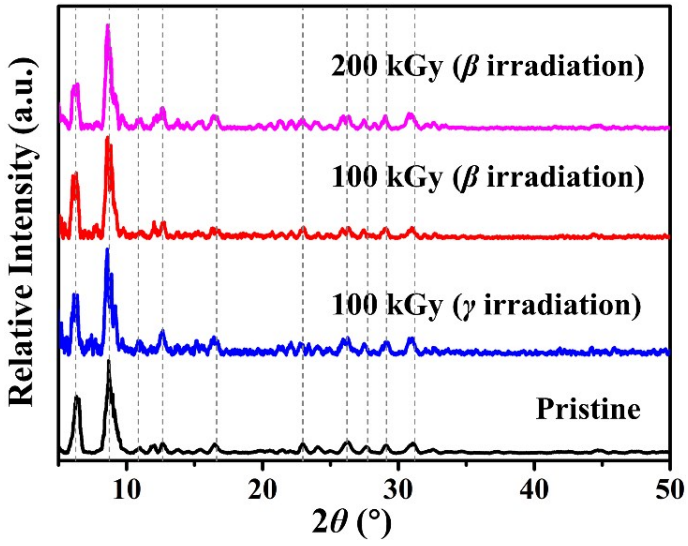

Figure S11. Powder XRD patterns of pristine **InS-1** and the corresponding samples after β and γ irradiation.

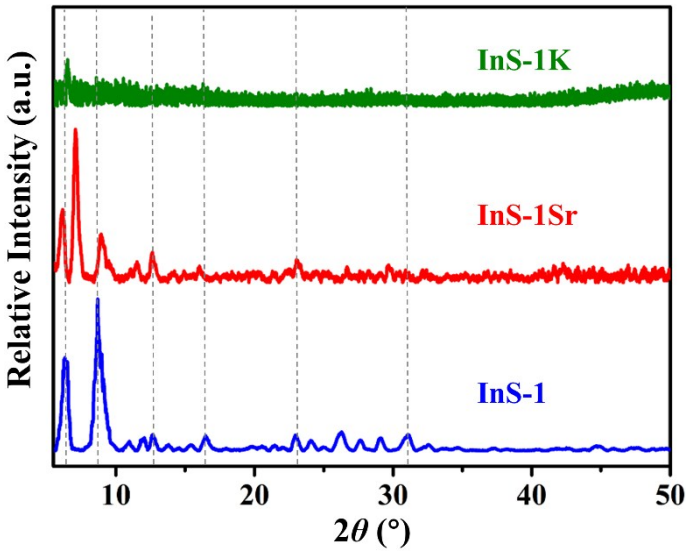

Figure S12. Powder XRD patterns of **InS-1**, **InS-1Sr** and the eluted product **InS-1K**.

References:

[1] Reflectance Spectroscopy; W. M. Wendlandt, H. G. Hecht, Eds.; Interscience: New York, **1966**.

[2] G. M. Sheldrick, A short history of SHELX, *Acta Crystallogr. Sect. A* **2008**, 64, 112-122.

[3] Adsorption analysis: Equilibria and kinetics; D. D. Do, Ed.; Imperial College Press: London, **1998**.

[4] M. J. Manos, C. D. Malliakas, M. G. Kanatzidis, Heavy-metal-ion capture, ion-exchange, and exceptional acid stability of the open-framework chalcogenide $(NH_4)_4In_{12}Se_{20}$. *Chem. Eur.*, *J.* **2007**, 13, 51-58.

[5] J.-R. Li, X.-Y. Huang, $[(Me)_2NH_2]_{0.75}[Ag_{1.25}SnSe_3]$: A three-dimensionally microporous chalcogenide exhibiting framework flexibility upon ion-exchange. *Dalton Trans.*, **2011**, 40, 4387-4390.

[6] H.-W. Liu, K.-Y. Wang, D. Ding, M. Sun, L. Cheng, C. Wang, Deep eutectic solvothermal synthesis of an open framework copper selenidogermanate with pH-resistant Cs^+ ion exchange properties. *Chem. Commun.*, **2019**, 55, 13884-13887.

[7] X.-M. Zhang, D. Sarma, Y.-Q. Wu, L. Wang, Z.-X. Ning, F.-Q. Zhang, M. G. Kanatzidis, Open-framework oxysulfide based on the supertetrahedral $[In_4Sn_{16}O_{10}S_{34}]^{12-}$ cluster and efficient sequestration of heavy metals. *J. Am. Chem. Soc.*, **2016**, 138, 5543-5546.

[8] N. Ding, M. G. Kanatzidis, Permeable layers with large windows in $[(CH_3CH_2CH_2)_2NH_2]_5In_5Sb_6S_{19}\cdot 1.45\ H_2O$: High ion-exchange capacity, size discrimination, and selectivity for Cs ions. *Chem. Mater.*, **2007**, 19, 3867-3869.

[9] B. Zhang, M.-L. Feng, H.-H. Cui, C.-F. Du, X.-H. Qi, N.-N. Shen, X.-Y. Huang, Syntheses, crystal structures, ion-exchange, and photocatalytic properties of two amine-directed Ge–Sb-S compounds. *Inorg. Chem.*, **2015**, 54, 8474-8481.

[10] N. Ding, M. G. Kanatzidis, Selective incarceration of caesium ions by venus flytrap action of a flexible framework sulfide. *Nat. Chem.*, **2010**, 2, 187-191.

[11] M.-L. Feng, D. Sarma, Y.-J. Gao, X.-H. Qi, W.-A. Li, X.-Y. Huang, M. G. Kanatzidis, Efficient removal of $[UO_2]^{2+}$, Cs^+, and Sr^{2+} ions by radiation-resistant gallium thioantimonates. *J. Am. Chem. Soc.*, **2018**, 140, 11133-11140.

[12] L. Wang, H. Pei, D. Sarma, X.-M. Zhang, K. M. Renaris, C. D. Malliakas, M. G. Kanatzidis, Highly selective radioactive $^{137}Cs^+$ capture in an open-framework oxysulfide based on supertetrahedral cluster. *Chem. Mater.*, **2019**, 31, 1628-1634.

[13] D. Sarma, C. D. Malliakas, K. S. Subrahmanyam, S. M. Islam and M. G. Kanatzidis, $K_{2x}Sn_{4-x}S_{8-x}$ (x = 0.65-1): a new metal sulfide for rapid and selective removal of Cs^+, Sr^{2+}, and UO_2^{2+} ions. *Chem. Sci.*, **2016**, 7, 1121-1132.

[14] X.-H. Qi, K.-Z. Du, M.-L. Feng, J.-R. Li, C.-F. Du, B. Zhang, X.-Y. Huang, A two-dimensionally microporous thiostannate with superior Cs^+, and Sr^{2+} ion-exchange property. *J. Mater. Chem. A.*, **2015**, 3, 5665-5673.

[15] M.-L. Feng, D. Sarma, X.-H. Qi, K.-Z. Du, X.-Y. Huang, Efficient removal and recovery of Uranium by a layered organic-inorganic hybrid thiostannate. *J. Am. Chem. Soc.*, **2016**, 138, 12578-12585.

[16] X.-H. Qi, K.-Z. Du, M.-L. Feng, Y.-J. Gao, X.-Y. Huang, M. G. Kanatzidis, Layered $A_2Sn_3S_7\cdot 1.25\ H_2O$ (A = organic cation) as efficient ion-exchanger for rare earth element recovery.

J. Am. Chem. Soc., **2017**, 139, 4314-4317.
[17] M. J. Manos, N. Ding, M. G. Kanatzidis, Layered metal sulfides: exceptionally selective agents for radioactive strontium removal. *Proc. Natl. Acad. Sci. U. S. A.* **2008**, 105, 3696-3699.
[18] M. J. Manos, M. G. Kanatzidis, Highly efficient and rapid Cs^+ uptake by the layered metal sulfide $K_{2x}Mn_xSn_{3-x}S_6$ (KMS-1). *J. Am. Chem. Soc.*, **2009**, 131, 6599-6607.
[19] M. J. Manos, M. G. Kanatzidis, Sequestration of heavy metals from water with layered metal sulfides. *Chem. Eur. J.* **2009**, 15, 4779-4784.
[20] M. J. Manos, M. G. Kanatzidis, Layered metal sulfides capture uranium from seawater. *J. Am. Chem. Soc.*, **2012**, 134, 16441-16446.
[21] J.-R. Li, X. Wang, B. Yuan, M.-L. Fu, Layered chalcogenide for Cu^{2+} removal by ion-exchange from wastewater. *J. Mol. Liq.*, **2014**, 200, 205-212.
[22] J. L. Mertz, Z. H. Fard, C. D. Malliakas, M. J. Manos, M. G. Kanatzidis, Selective removal of Cs^+, Sr^{2+}, and Ni^{2+} by $K_{2x}Mg_xSn_{3-x}S_6$ (x = 0.5-1) (KMS-2) relevant to nuclear waste remediation. *Chem. Mater.*, **2013**, 25, 2116-2127.
[23] M.-L. Feng, D.-N. Kong, Z.-L. Xie, X.-Y. Huang, Three-dimensional chiral microporous germanium antimony sulfide with ion-exchange properties. *Angew. Chem. Int. Ed.*, **2008**, 47, 8623-8626.
[24] M. J. Manos, R. G. Iyer, E. Quarez, J. H. Liao, M. G. Kanatzidis, $\{Sn[Zn_4Sn_4S_{17}]\}^{6-}$: a robust open framework based on metal-linked penta-supertetrahedral $[Zn_4Sn_4S_{17}]^{10-}$ clusters with ion-exchange properties. *Angew. Chem. Int. Ed.*, **2009**, 48, 7871-7874.
[25] M. J. Manos, K. Chrissafis, M. G. Kanatzidis, Unique pore selectivity for Cs^+ and exceptionally high NH_4^+ exchange capacity of the chalcogenide material $K_6Sn[Zn_4Sn_4S_{17}]$. *J. Am. Chem. Soc.*, **2006**, 128, 8875-8883.
[26] K.-Y. Wang, M.-L. Feng, J.-R. Li, X.-Y. Huang, $[NH_3CH_3]_4[In_4SbS_9SH]$: a novel methylamine-directed indium thioantimonate with Rb^+ ion-exchange property. *J. Mater. Chem. A.*, **2013**, 1, 1709-1715.
[27] K.-Y. Wang, D. Ding, M. Sun, L. Cheng, C. Wang, Effective and rapid adsorption of Sr^{2+} ions by a hydrated pentasodium cluster templated zinc thiostannate. *Inorg. Chem.*, **2019**, 58, 10184-10193.